

Flavored Leptogenesis and Neutrino Mass with A_4 symmetry

Arghyajit Datta,^a Biswajit Karmakar,^{b,c} Arunansu Sil^a

^a*Department of Physics, Indian Institute of Technology Guwahati, Assam-781039, India*

^b*Department of Physics, Indian Institute of Technology Hyderabad, 502285 Telangana, India*

^c*Institute of Physics, University of Silesia, 40-007 Katowice, Poland*

E-mail: datta176121017@iitg.ac.in, biswajit.karmakar@us.edu.pl,
asil@iitg.ac.in

ABSTRACT: We propose a minimal A_4 flavor symmetric model, assisted by $Z_2 \times Z_3$ symmetry, which can naturally takes care of the appropriate lepton mixing and neutrino masses via Type-I seesaw. It turns out that the framework, originated due to a specific flavor structure, favors the normal hierarchy of light neutrinos and simultaneously narrows down the range of Dirac CP violating phase. It predicts an interesting correlation between the atmospheric mixing angle and the Dirac CP phase too. While the flavor structure indicates an exact degeneracy of the right-handed neutrino masses, renormalization group running of the same from a high scale is shown to make it quasi-degenerate and a successful flavor leptogenesis takes place within the allowed parameter space obtained from neutrino phenomenology.

ARXIV EPRINT: [2106.06773](https://arxiv.org/abs/2106.06773)

Contents

1	Introduction	1
2	Structure of The Model	3
3	Neutrino phenomenology	8
3.1	Constraining the parameter space	8
3.2	Implications for light neutrino masses and low energy phase	10
3.3	Neutrinoless Double beta decay	11
3.4	Lepton flavor violation	12
4	Leptogenesis	12
4.1	Generation of mass splitting and CP asymmetry	13
4.1.1	Lifting the mass degeneracy	14
4.1.2	Estimating CP asymmetry	16
4.2	Solution of Boltzmann equation	18
5	Conclusion	21
A	A_4 Multiplication Rules:	22

1 Introduction

Over the last couple of decades, we have witnessed remarkable success in neutrino experiments [1–9] indicating that neutrinos are indeed massive. Furthermore, mixing parameters have been measured with great precision. In fact, two of the three mixing angles namely solar (θ_{12}) and atmospheric (θ_{23}) ones are found to be large while the other one, reactor (θ_{13}) mixing angle, is relatively small. Such a finding clearly shows the distinctive feature associated to the lepton sector in contrast to the quark one where all the three mixing angles are measured to be small. To have a deeper understanding of it, one needs to investigate the origin of the neutrino mass by looking at the neutrino mass matrix as well as the charged lepton sector from a symmetry perspective.

To address the tiny neutrino mass issue, various seesaw mechanisms [10–17] have been proposed by extending the Standard Model (SM) with heavy fermions/scalars. Among these, the type-I seesaw mechanism provides perhaps the simplest explanation of tiny neutrino mass where the SM is extended by three singlet right-handed neutrinos (RHN) [10–12]. Involvement of flavor symmetries within this simple setup is off course an interesting possibility in order to explain the typical mixing pattern in the lepton sector. Non-abelian discrete groups (like $S_3, A_4, S_4, A_5, \Delta(27)$ etc.) in this regard have been extensively used (see reviews [18–25] and references therein).

Among the various discrete groups, A_4 turns out to be the most economical one¹. It is a group of even permutations of four objects having three inequivalent one-dimensional representations (1, 1' and 1'') as well as one three-dimensional representation (3). Interestingly, the three generations (or flavors) of right-handed charged lepton singlets can naturally fit into these three inequivalent one-dimensional representations of A_4 while the three SM lepton doublets can be accommodated into the triplet representation of A_4 [28–30]. Works along this direction [28, 29, 31, 32] showed that type-I seesaw model with A_4 flavor symmetry in general leads to a typical tri-bimaximal (TBM) lepton mixing ($\sin^2 \theta_{12} = 1/3$, $\sin^2 \theta_{23} = 1/2$ and $\theta_{13} = 0$) pattern [33, 34] in presence of SM singlet (though charged under A_4) flavon fields. Though such TBM pattern received a great deal of attention due to its close proximity with experimental observation prior to 2012, it fails to accommodate the recent observation of small, but non-zero θ_{13} [8, 35, 36]. Subsequently, modifications over models based on A_4 (and other discrete groups) are suggested to accommodate non-zero θ_{13} either by considering additional flavon fields or including corrections to vacuum alignments of the flavons [37, 38] or considering contributions to additional mixing from the charged lepton sector [39].

In this work, we particularly focus on a framework where a non-trivial contribution to lepton mixing is originated from charged lepton sector. We do not consider any additional flavon field apart from those ones incorporated in the original Altarelli-Feruglio (AF) model [28]. While the RHN mass matrix turns out to be diagonal as a result of the flavor symmetry imposed, the structure of the charged lepton mass matrix becomes such that it can be diagonalized by a complex ‘magic’ matrix [29]. Interestingly, an antisymmetric contribution to the Dirac neutrino mass matrix, originated from the product of two A_4 triplets, plays a crucial role in generating non-zero θ_{13} [40–43] in our model which was overlooked in an earlier attempt [44]. In doing the analysis, we find the atmospheric mixing angle $\theta_{23} \leq 45^\circ$ *i.e.* to lie in lower octant (LO). We also note that only normal hierarchy (NH) of light neutrino masses are allowed in this model. This turns out to be another salient feature of our construction. These predictions can be tested in ongoing and future neutrino experiments as ambiguities are still present in determining octant for θ_{23} as well as hierarchies of light neutrino masses.

Additionally, we also discuss the aspects of leptogenesis [45–49] from the CP-violating decays of RHNs in this A_4 based type-I seesaw scenario in line with observations [50–57]. In doing so, since the involvement of the neutrino Yukawa matrix in the charged-lepton mass diagonal basis is necessary, the specific flavor symmetric construction of it is expected to play an important role. In fact, due to this symmetry, exactly degenerate heavy RHNs result at tree level, thereby indicating the breaking of the perturbative field theory involved in CP asymmetry generation [58]. Following [44], we are able to show that running of the parameters involved in the neutrino sector from the flavor symmetry breaking scale to the RHN mass scale actually eliminates such exact degeneracies and as a result, leptogenesis can indeed be possible. The present study of matter-antimatter asymmetry generation via leptogenesis taking into account the effect of running however differs from that of [44] by

¹ A_4 group was initially proposed as an underlying family symmetry for quark sector by [26, 27].

two aspects. Firstly, we use less number of flavon fields and secondly, we present a detailed analysis of flavored leptogenesis by solving the relevant Boltzmann equations.

The rest of the paper is organized as follows. In Section 2 we present detail structure of the model including the analysis of the mixing matrices involved. Section 3 deals with phenomenology of neutrino mixing. Constrains and predictions on neutrino parameters (including neutrinoless double beta decay) involved are presented here. In Section 4 we perform a detailed study on leptogenesis solving flavored Boltzmann equations. Finally in Section 5 we summarize the results and make final conclusion.

2 Structure of The Model

To realize the canonical type-I seesaw mechanism, we first consider an extension of the SM by including three singlet RHN fields (N_R). Additionally, three flavon fields namely Φ , Ψ , φ and a discrete symmetry $A_4 \times Z_2 \times Z_3$ are also incorporated to probe the typical flavor structure involved in the lepton sector. Note that same fields content was also present in the original AF [18] construction. Here N_R and the flavon fields Φ , Ψ transform as triplet, whereas φ transforms as a singlet under A_4 . A judicious choice of additional $Z_2 \times Z_3$ symmetry assists the leptonic mass matrices to take specific forms and hence forbid several unwanted contributions. In Table 1, we present transformation properties of all the relevant SM fields, N_R and flavons involved in the analysis.

Fields	ℓ	e_R	μ_R	τ_R	N_R	H	φ	Φ	Ψ
SM	$(2, 1/2)$	$(1, 1)$	$(1, 1)$	$(1, 1)$	$(1, 0)$	$(2, -1/2)$	$(1, 0)$	$(1, 0)$	$(1, 0)$
A_4	3	1	1'	1''	3	1	1	3	3
Z_2	1	1	1	1	-1	1	-1	1	-1
Z_3	ω	1	1	1	1	1	ω	ω	ω

Table 1: Representations of the fields under $SU(2)_L \times U(1)_Y \times A_4 \times Z_2 \times Z_3$ symmetry

The relevant effective Lagrangian involving charged leptons and neutrinos can be written as

$$\begin{aligned}
\mathcal{L} \supset & \frac{y_1^\ell}{\Lambda} (\bar{\ell} \Phi)_1 H e_R + \frac{y_2^\ell}{\Lambda} (\bar{\ell} \Phi)_{1''} H \mu_R + \frac{y_3^\ell}{\Lambda} (\bar{\ell} \Phi)_{1'} H \tau_R \\
& + \frac{y_1^\nu}{\Lambda} [(\bar{\ell} N_R)_s \Psi]_1 \tilde{H} + \frac{y_2^\nu}{\Lambda} [(\bar{\ell} N_R)_a \Psi]_1 \tilde{H} + \frac{y_3^\nu}{\Lambda} (\bar{\ell} N_R)_1 \varphi \tilde{H} + \frac{1}{2} M (\bar{N}_R^c N_R) + \text{h.c.},
\end{aligned}
\tag{2.1}$$

where $y_{i=1,2,3}^{\ell,\nu}$ are the respective coupling constants, M is the mass parameter of RHNs and Λ is the cut-off scale of the theory. In the first line of Eq. (2.1), terms in the first parentheses represent products of two A_4 triplets forming a one-dimensional representation which further contract with 1, 1' and 1'' of A_4 , corresponding to e_R , μ_R and τ_R respectively, to make a true singlet under A_4 . On the other hand, in the second line of Eq. (2.1), the subscripts **s**, **a** correspond to symmetric and anti-symmetric parts of triplet products in

the S diagonal basis of A_4 . The essential multiplication rules of the A_4 group elements are elaborated in appendix A.

From Table 1 it is evident that the tree level contribution to charged lepton Yukawa interaction, $\bar{\ell} H \alpha_R$ (with $\alpha = e, \mu, \tau$), gets forbidden. Instead, such interactions are effectively generated once the flavon Φ gets a vacuum expectation value (vev) via the dimension-5 operators (present in first line of Eq. (2.1)). Similarly in the neutrino sector, the renormalizable Dirac Yukawa coupling is forbidden as the lepton doublet ℓ is charged under Z_3 whereas both N_R and H transform trivially under it. However such effective Yukawa coupling is generated from dimension-5 operators involving flavons Ψ and φ , after they obtain vevs. Presence of Z_2 symmetry is important in identifying Φ from Ψ (both being A_4 triplet) so that they contribute to the charged lepton and Dirac neutrino Yukawa couplings differently.

The flavon fields break the flavor symmetry $A_4 \times Z_3 \times Z_2$ when they acquire vevs along²

$$\langle \varphi \rangle = v_\varphi, \langle \Phi \rangle = v_\Phi (1, 1, 1), \langle \Psi \rangle = v_\Psi (0, 1, 0), \quad (2.2)$$

as a result of which the part of the Lagrangian contributing to the charged lepton sector can be written as

$$\mathcal{L}_l = \frac{y_1^\ell v_\Phi}{\Lambda} (\bar{\ell}_e + \bar{\ell}_\mu + \bar{\ell}_\tau) H e_R + \frac{y_2^\ell v_\Phi}{\Lambda} (\bar{\ell}_e + \omega \bar{\ell}_\mu + \omega^2 \bar{\ell}_\tau) H \mu_R + \frac{y_3^\ell v_\Phi}{\Lambda} (\bar{\ell}_e + \omega^2 \bar{\ell}_\mu + \omega \bar{\ell}_\tau) H \tau_R. \quad (2.3)$$

Using the above Lagrangian one obtains the charged lepton mass matrix after the electroweak symmetry breaking as

$$Y^\ell = v \begin{pmatrix} f_1^\ell & f_2^\ell & f_3^\ell \\ f_1^\ell & \omega f_2^\ell & \omega^2 f_3^\ell \\ f_1^\ell & \omega^2 f_2^\ell & \omega f_3^\ell \end{pmatrix}; \quad f_i^\ell = \frac{v_\Phi}{\Lambda} y_i^\ell \text{ with } i = 1, 2, 3, \quad (2.4)$$

where $v = 174$ GeV stands for the vev of the SM Higgs.

In a similar way, the Lagrangian for neutrino sector after breaking of the flavor symmetries can be written as

$$\begin{aligned} \mathcal{L}_\nu = & \frac{y_3^\nu}{\Lambda} v_\varphi (\bar{\ell}_e N_{1R} + \bar{\ell}_\mu N_{2R} + \bar{\ell}_\tau N_{3R}) \tilde{H} + (y_1^\nu - y_2^\nu) \frac{v_\Psi}{\Lambda} \bar{\ell}_e N_{3R} \tilde{H} \\ & + (y_1^\nu + y_2^\nu) \frac{v_\Psi}{\Lambda} \bar{\ell}_\tau N_{1R} \tilde{H} + M (\bar{N}_{1R}^c N_{1R} + \bar{N}_{2R}^c N_{2R} + \bar{N}_{3R}^c N_{3R}) + \text{h.c.} \end{aligned} \quad (2.5)$$

This yields the corresponding Dirac and Majorana mass matrices as

$$Y^\nu = \begin{pmatrix} f_3^\nu & 0 & f_1^\nu - f_2^\nu \\ 0 & f_3^\nu & 0 \\ f_1^\nu + f_2^\nu & 0 & f_3^\nu \end{pmatrix}, \quad (2.6)$$

$$M_R = \begin{pmatrix} M & 0 & 0 \\ 0 & M & 0 \\ 0 & 0 & M \end{pmatrix}, \quad (2.7)$$

²Such vev alignments of the flavons is widely used and can be realised in a natural way by minimising the scalar potential following the approach of [18, 40, 44, 59–62].

with $f_i^\nu = \frac{v_\Psi}{\Lambda} y_i^\nu$, $i = 1, 2, 3$.

Let us now discuss the diagonalization of the charged lepton and neutrino mass matrices so as to obtain the lepton mixing matrix. First we note that the charged lepton mass matrix given in Eq. (2.4) can be diagonalized by a bi-unitary transformation

$$Y^\ell = V d^\ell \mathbb{I}_{3 \times 3} \text{ with } d^\ell = \sqrt{3}v \text{diag}(f_1^\ell, f_2^\ell, f_3^\ell), \quad (2.8)$$

where $\mathbb{I}_{3 \times 3}$ is a 3×3 identity matrix and

$$V = \frac{1}{\sqrt{3}} \begin{pmatrix} 1 & 1 & 1 \\ 1 & \omega & \omega^2 \\ 1 & \omega^2 & \omega \end{pmatrix}, \quad (2.9)$$

where $\omega (= e^{2i\pi/3})$ is the cube root of unity. From Eq. (2.7), it is evident that the right-handed Majorana neutrino mass matrix M_R is diagonal having degenerate mass eigenvalues (M) to start with.

On the other hand, f_1^ν and f_2^ν appearing in Eq. (2.6) are the symmetric and anti-symmetric contributions to the Dirac neutrino Yukawa respectively, originated as products of two A_4 triplets ℓ and N_R which further contract with Φ (see the product rules Eq. (A.5) and (A.6)). This antisymmetric part plays an instrumental role³ in realizing correct neutrino oscillation data.

Here it is worth mentioning that in the vanishing limit of $f_2^\nu \rightarrow 0$, (keeping the structure of the charged lepton and Majorana mass matrix intact) one can reproduce the TBM mixing as discussed in [44].

The effective light neutrino mass⁴ matrix can be obtained within the type-I seesaw framework as

$$m_\nu = -m_D M_R^{-1} m_D^T, \quad (2.10)$$

where the structure of M_R is given in Eq. (2.7). Now, from Eq. (2.6) and (2.8), in the basis where the charged leptons are diagonal, the Dirac neutrino mass matrix in that basis can be written as,

$$m_D = v V^\dagger Y^\nu = v \mathcal{Y}^\nu. \quad (2.11)$$

Therefore, substituting Eq. (2.11) in the type-I seesaw formula given by Eq. (2.10) one obtains the light neutrino mass matrix as

$$m_\nu = -v^2 V^\dagger Y^\nu M_R^{-1} Y^{\nu T} V^*, \quad (2.12)$$

$$= -\frac{1}{M} V^\dagger (v^2 Y^\nu Y^{\nu T}) V^*. \quad (2.13)$$

³Earlier the role of such antisymmetric contributions was analyzed in the context of Dirac neutrinos [40–43].

⁴With the symmetries mentioned in Table 1 in principle, there will be a contribution to the effective light neutrino mass via a dim-6 operator given by $\frac{v_{eff}}{\Lambda^2} (\ell H \ell H \Phi)$. However, in the limit $v_\Phi > M$, this additional contribution can be neglected compared to the dominant type-I contribution considered here.

Clearly, to get the mass eigenvalues of light neutrinos we need to diagonalize $Y^\nu Y^{\nu T}$ where

$$Y^\nu Y^{\nu T} = \begin{pmatrix} (f_1^\nu - f_2^\nu)^2 + f_3^{\nu^2} & 0 & 2f_1^\nu f_3^\nu \\ 0 & f_3^{\nu^2} & 0 \\ 2f_1^\nu f_3^\nu & 0 & (f_1^\nu + f_2^\nu)^2 + f_3^{\nu^2} \end{pmatrix}. \quad (2.14)$$

Though Y^ν is in general a complex matrix, $Y^\nu Y^{\nu T}$ being a complex symmetric matrix can be diagonalized by an orthogonal transformation (in the $(1, 3)$ plane) through the relation

$$U_{13}^T (Y^\nu Y^{\nu T}) U_{13} = d_D^2 = \text{diag}(\lambda_1, \lambda_2, \lambda_3), \quad (2.15)$$

where the rotation matrix U_{13} (parametrised by angle θ and phase ψ) is given by

$$U_{13} = \begin{pmatrix} \cos \theta & 0 & e^{-i\psi} \sin \theta \\ 0 & 1 & 0 \\ -e^{i\psi} \sin \theta & 0 & \cos \theta \end{pmatrix}. \quad (2.16)$$

The complex eigenvalues are given by

$$\lambda_1 = f_1^{\nu^2} + f_2^{\nu^2} + f_3^{\nu^2} - 2\sqrt{f_1^{\nu^2}(f_2^{\nu^2} + f_3^{\nu^2})}, \quad (2.17)$$

$$\lambda_2 = f_3^{\nu^2}, \quad (2.18)$$

$$\lambda_3 = f_1^{\nu^2} + f_2^{\nu^2} + f_3^{\nu^2} + 2\sqrt{f_1^{\nu^2}(f_2^{\nu^2} + f_3^{\nu^2})}. \quad (2.19)$$

Now substituting Eq. (2.15) in Eq. (2.13), we get

$$m_\nu = -V^\dagger U_{13} \left(\frac{v^2 d_D^2}{M} \right) U_{13}^T V^*, \quad (2.20)$$

$$= -V^\dagger U_{13} (d_\nu) U_{13}^T V^*, \quad (2.21)$$

where $d_\nu = v^2 d_D^2 / M$ is a diagonal matrix having diagonal elements $v^2 \lambda_i / M$ ($i = 1, 2, 3$), representative of three complex light neutrino mass eigenvalues.

In order to extract the real and positive light neutrino mass eigenvalues, we choose the following representations of the parameters $f_{1,2,3}^\nu (= |f_{1,2,3}^\nu| e^{i\phi_{1,2,3}}$ and $\phi_{1,2,3}$ are the three phases associated) as

$$\frac{f_1^\nu}{f_3^\nu} = \frac{|f_1^\nu|}{|f_3^\nu|} e^{i(\phi_1 - \phi_3)} = \chi_1 e^{i\gamma_1}, \quad (2.22)$$

$$\frac{f_2^\nu}{f_3^\nu} = \frac{|f_2^\nu|}{|f_3^\nu|} e^{i(\phi_2 - \phi_3)} = \chi_2 e^{i\gamma_2}, \quad (2.23)$$

where $\chi_1 = |f_1^\nu / f_3^\nu|$, $\chi_2 = |f_2^\nu / f_3^\nu|$ and $(\phi_1 - \phi_3) = \gamma_1$, $(\phi_2 - \phi_3) = \gamma_2$ are the redefined parameters used for the rest of our analysis.

Now we are in a position to define the rotation angle θ and phase ψ of U_{13} matrix (see Eq. (2.16)) as:

$$\tan 2\theta = \frac{2\chi_1}{2\chi_1\chi_2 \cos \gamma_2 \cos \psi - [\chi_1^2 \sin \gamma_1 + \chi_2^2 \sin(2\gamma_2 - \gamma_1) - \sin \gamma_1] \sin \psi}, \quad (2.24)$$

$$\tan \psi = \frac{-2\chi_1\chi_2 \sin \gamma_2}{\cos \gamma_1 + \chi_2^2 \cos(2\gamma_2 - \gamma_1) + \chi_1^2 \cos \gamma_1}. \quad (2.25)$$

Similarly, the real and positive light neutrino masses can also be expressed in terms of $\chi_{1,2}$ and $\gamma_{1,2}$ after we extract the phases from the complex eigenvalues. To proceed, note that Eq. (2.21) can be rewritten as

$$m_\nu \equiv U \text{diag}(m_1, m_2, m_3) U^T, \quad (2.26)$$

with

$$U = V^\dagger U_{13} e^{i\frac{\pi}{2}} U_p. \quad (2.27)$$

Here U_p stands for a diagonal phase matrix given by $U_p = \text{diag}(1, e^{i\beta_{21}/2}, e^{i\beta_{31}/2})$, and the real positive light neutrino masses are given by:

$$m_1 = \frac{v^2}{M} |f_3^{\nu^2}| \sqrt{o_r^2 + o_i^2}, \quad (2.28)$$

$$m_2 = \frac{v^2}{M} |f_3^{\nu^2}|, \quad (2.29)$$

$$m_3 = \frac{v^2}{M} |f_3^{\nu^2}| \sqrt{n_r^2 + n_i^2}, \quad (2.30)$$

where o_r, o_i, n_r and n_i can be written in terms of the associated parameters (χ_1, χ_2, γ_1 and γ_2) in our model as

$$o_r = \chi_1^2 \cos 2\gamma_1 + \chi_2^2 \cos 2\gamma_2 + 1 - 2A\chi_1 \cos \gamma_1 + 2B\chi_1 \sin \gamma_1, \quad (2.31)$$

$$o_i = \chi_1^2 \sin 2\gamma_1 + \chi_2^2 \sin 2\gamma_2 - 2A\chi_1 \sin \gamma_1 - 2B\chi_1 \cos \gamma_1, \quad (2.32)$$

$$n_r = \chi_1^2 \cos 2\gamma_1 + \chi_2^2 \cos 2\gamma_2 + 1 + 2A\chi_1 \cos \gamma_1 - 2B\chi_1 \sin \gamma_1, \quad (2.33)$$

$$n_i = \chi_1^2 \sin 2\gamma_1 + \chi_2^2 \sin 2\gamma_2 + 2A\chi_1 \sin \gamma_1 + 2B\chi_1 \cos \gamma_1, \quad (2.34)$$

$$A = \frac{\sqrt{1 + \chi_2^2 \cos 2\gamma_2 + \sqrt{1 + \chi_2^4 + 2\chi_2^2 \cos 2\gamma_2}}}{\sqrt{2}}, B = \frac{\chi_2^2 \sin 2\gamma_2}{2A}. \quad (2.35)$$

The phases $\beta_{21(31)}$ involved in U_p are given by,

$$\beta_{21} = -\tan^{-1} \frac{o_i}{o_r}, \beta_{31} = \tan^{-1} \frac{n_i}{n_r} - \tan^{-1} \frac{o_i}{o_r}. \quad (2.36)$$

Therefore using Eqs. (2.9), (2.16) and (2.27), the final form of the mixing matrix U which diagonalises the effective light neutrino mass matrix (in the charged lepton diagonal basis) can now be written as

$$U = \begin{pmatrix} \frac{\cos \theta - e^{i\psi} \sin \theta}{\sqrt{3}} & \frac{1}{\sqrt{3}} & \frac{\cos \theta + e^{-i\psi} \sin \theta}{\sqrt{3}} \\ \frac{\cos \theta - \omega e^{i\psi} \sin \theta}{\sqrt{3}} & \frac{\omega^2}{\sqrt{3}} & \frac{\omega \cos \theta + e^{-i\psi} \sin \theta}{\sqrt{3}} \\ \frac{\cos \theta - \omega^2 e^{i\psi} \sin \theta}{\sqrt{3}} & \frac{\omega}{\sqrt{3}} & \frac{\omega^2 \cos \theta + e^{-i\psi} \sin \theta}{\sqrt{3}} \end{pmatrix} e^{i\pi/2} U_p. \quad (2.37)$$

parameters	best fit value	3σ range
$\sin^2 \theta_{12}$	0.304	$0.269 \rightarrow 0.343$
$\sin^2 \theta_{23}$	0.573	$0.415 \rightarrow 0.616$
$\sin^2 \theta_{13}$	0.02219	$0.02032 \rightarrow 0.02410$
$\delta_{CP}/^\circ$	197	$120 \rightarrow 369$
$\frac{\Delta m_{21}^2}{10^{-5} \text{ eV}^2}$	7.42	$6.82 \rightarrow 8.04$
$\frac{\Delta m_{31}^2}{10^{-3} \text{ eV}^2}$	+2.517	$+2.435 \rightarrow +2.598$

Table 2: neutrino oscillation data obtained from NuFIT[64] for NH scenario of light neutrino mass.

U is therefore the lepton mixing matrix, called the Pontecorvo-Maki-Nakagawa-Sakata (U_{PMNS}) matrix, the standard form of which is given by [63],

$$U_{PMNS} = \begin{pmatrix} c_{12}c_{13} & s_{12}c_{13} & e^{-i\delta}s_{13} \\ -s_{12}s_{23} - e^{i\delta}c_{12}s_{13}s_{23} & c_{12}c_{23} - e_{i\delta}s_{12}s_{13}s_{23} & c_{13}s_{23} \\ s_{12}s_{23} - e^{i\delta}c_{12}s_{13}s_{23} & -c_{12}c_{23} - e_{i\delta}s_{12}s_{13}s_{23} & c_{13}c_{23} \end{pmatrix} U_m, \quad (2.38)$$

where $c_{ij} = \cos \theta_{ij}$ and $s_{ij} = \sin \theta_{ij}$, and δ is the CP violating Dirac phase. Also, $U_m = \text{diag}(1, e^{i\alpha_{21}/2}, e^{i\alpha_{31}/2})$ is a phase matrix which contains two Majorana phases α_{21} and α_{31} . Comparing above two matrices given in Eq. (2.37) and (2.38) we get the correlation between the neutrino mixing angles (and Dirac CP phase) appearing in U_{PMNS} and the model parameters as [40]

$$|s_{13}|^2 = \frac{1 + \sin 2\theta \cos \psi}{3}, \quad \tan \delta = \frac{\sin \theta \sin \psi}{\cos \theta + \sin \theta \cos \psi}, \quad (2.39)$$

$$s_{12}^2 = \frac{1}{3(1 - |s_{13}|^2)}, \quad \tan 2\theta_{23} \cos \delta = \frac{1 - 2|s_{13}|^2}{|s_{13}| \sqrt{2 - 3|s_{13}|^2}}. \quad (2.40)$$

Additionally, the two Majorana phases α_{21} and α_{31} are identified as $\alpha_{21} = \beta_{21}$, and $\alpha_{31} = \beta_{31}$ (ignoring the irrelevant common phase). These correlations given in Eq. (2.39)-(2.40) are the keys to the subsequent analysis of neutrino phenomenology.

3 Neutrino phenomenology

3.1 Constraining the parameter space

As seen from Eqs. (2.39) and (2.40) in conjugation with Eqs. (2.24) and (2.25), all the mixing angles ($\theta_{13}, \theta_{12}, \theta_{23}$) and the Dirac CP phase (δ) involved in the lepton mixing matrix U_{PMNS} are finally determined by the model parameters χ_1, χ_2, γ_1 and γ_2 . Hence, using the 3σ allowed ranges of the three mixing angles ($\theta_{13}, \theta_{12}, \theta_{23}$) from neutrino oscillation data⁵ presented in Table 2, we can restrict parameter space for $\chi_{1,2}$ and $\gamma_{1,2}$. This parameter space of the current set-up can be further constrained using the 3σ allowed ranges of the

⁵The Majorana phases are insensitive to neutrino oscillation experiments. However, they may play an important role in neutrinoless double beta decay [65].

mass-squared differences (see Table 2). For that purpose, we introduce a dimensionless quantity r , defined as the ratio of solar to atmospheric mass squared difference for normal hierarchy, *i.e.*, $r = \frac{\Delta m_{21}^2}{\Delta m_{31}^2}$ with $\Delta m_{21}^2 = m_2^2 - m_1^2$ and $\Delta m_{31}^2 = m_3^2 - m_1^2$. Using the three light neutrino mass eigenvalues given in Eq. (2.28)-(2.30), we are able to rewrite it as

$$r = \frac{\Delta m_{21}^2}{\Delta m_{31}^2} = \frac{1 - o_r^2 - o_i^2}{n_r^2 + n_i^2 - o_r^2 - o_i^2}. \quad (3.1)$$

Substituting $o_{r,i}, n_{r,i}$ from Eq. (2.31)-(2.34) into Eq. (3.1), we note that r now becomes function of χ_1, χ_2, γ_1 and γ_2 . Apart from the satisfaction of r value obtained from the ratio of the best fit values of mass-squared differences, we must satisfy both the individual mass-squared differences, Δm_{21}^2 and Δm_{31}^2 , independently within their 3σ allowed ranges using Eqs. 2.28-2.30. There also exists a cosmological upper bound on sum of the light neutrinos masses as $\sum_i m_i \leq 0.11$ eV [66, 67] which will also constrain the parameter space. Note that in order to evaluate $\sum_i m_i$, we need to get an estimate of the pre-factor $|f_3^{\nu^2}|v^2/M$ (see Eqs. (2.28)-(2.30)) which can be obtained by using the relation

$$|f_3^{\nu^2}|v^2/M = \sqrt{\Delta m_{21}^2/(1 - o_r^2 - o_i^2)}, \quad (3.2)$$

with the known value of Δm_{21}^2 from current global analysis [64].

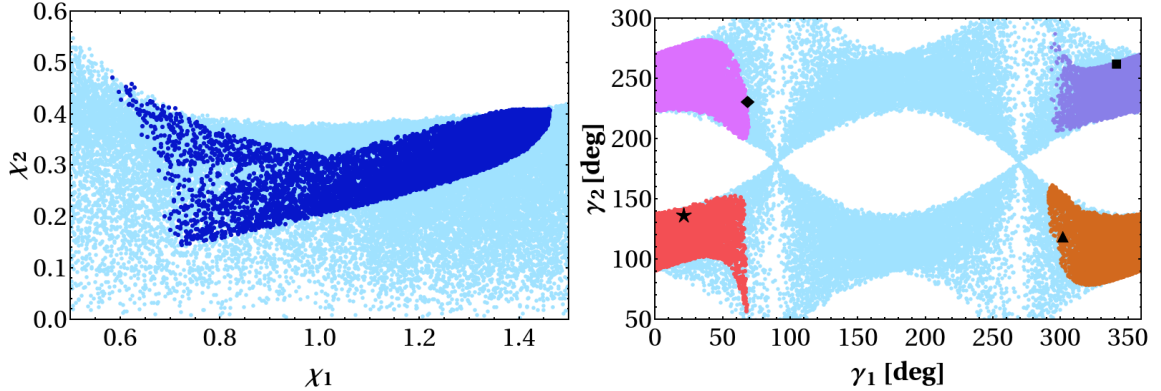


Figure 1: Allowed parameter spaces of χ_1 - χ_2 (left panel) and γ_1 - γ_2 (right panel) using 3σ ranges of neutrino oscillation parameters [64]. The light blue dots in both the panels correspond to 3σ allowed values for the mixing angles while the darker patches in each panel further satisfy constraints coming from the mass-squared differences, their ratio and sum of absolute masses. ★, ▲, ■, ◆ marks of the right panel are indicative of four benchmark points (BP) used in Section 4.

Equipped with all these, we provide a range of the allowed parameter space of our model in Fig. 1. In the left panel, we first indicate the correlation between two of the parameters $\chi_1 - \chi_2$ while the same for $\gamma_1 - \gamma_2$ is shown in the right panel, indicated by the light blue points. The corresponding values of the parameters (light blue points)

satisfy the 3σ allowed ranges of the lepton mixing angles, $\theta_{13}, \theta_{12}, \theta_{23}$. In obtaining these points, we varied parameters within a large range. For example, $\chi_{1,2}$ are varied from 0 to 2 while $\gamma_{1,2}$ are considered within their full range: $0-360^\circ$. Once we also incorporate the constraints following from the mass-squared differences as well as the one on the sum of the light neutrino masses, the entire allowed parameter space is reduced to a smaller region indicated by the dark blue patch on the left panel (in $\chi_1 - \chi_2$ plane) and four cornered patches (red, magenta, brown and purple) on the right panel (in $\gamma_1 - \gamma_2$ plane).

From Fig. 1, we find $0.584 \lesssim \chi_1 \lesssim 1.462$ whereas the ratio of the magnitudes of the antisymmetric contribution to the diagonal one (in view of Eq. (2.6)) falls in a range: $0.470 \gtrsim \chi_2 \gtrsim 0.145$. Turning into the right panel, we find that γ_1 and γ_2 both are pushed toward four cornered regions represented by red, magenta, brown and purple patches respectively. Here we find that for $0^\circ \leq \gamma_1 \leq 69^\circ$ the allowed regions for γ_2 are $(57^\circ - 152^\circ)$ and $(200^\circ - 282^\circ)$. Whereas for $291^\circ \leq \gamma_1 \leq 360^\circ$, the allowed regions for γ_2 are limited within $(78^\circ - 161^\circ)$ and $(206^\circ - 287^\circ)$. Here we also note that, in the right panel of Fig. 1, $\star, \blacktriangle, \blacksquare$ and \blacklozenge represent four unique benchmark points in the parameter space $\{\chi_1, \chi_2, \gamma_1, \gamma_2\}$ given by BP1 = (1.37, 0.399, 21.53° , 135.59°), BP2 = (0.978, 0.235, 301.81° , 119.1°), BP3 = (1.417, 0.372, 341.6° , 260.83°) and BP4 = (0.707, 0.209, 68.62° , 231.15°). It is important to note that so far the analysis presented here is applicable only for normal hierarchy of light neutrino mass. In the present setup, due to the special flavor structure of the model an inverted hierarchy of light neutrino mass spectrum however can not be accommodated. This is an interesting prediction that will undergo tests in several ongoing and near-future experiments.

3.2 Implications for light neutrino masses and low energy phase

From the previous part of the analysis, we have an understanding on the allowed regions for the χ_1, χ_2, γ_1 and γ_2 which satisfy all the constraints in the form of mass square differences, mixing angles and sum of the light neutrino masses. Hence, we are now in a position to study the implications of this allowed parameter space toward the predictions involving sum of the light neutrino masses, and phases. We already have correlation between the Dirac CP phase δ and the atmospheric mixing angle θ_{23} as seen from Eqs. (2.39) and (2.40), both of which are functions of $\chi_{1,2}, \gamma_{1,2}$ as evident from Eqs. (2.24), (2.25). In Fig. 2a, we have plotted this correlation in $\delta - \theta_{23}$ plane where only the allowed set of points for χ_1, χ_2, γ_1 and γ_2 are employed (as in Fig. 1). The model seems to predict δ to be in the range $33^\circ(213^\circ) \lesssim \delta \lesssim 80^\circ(260^\circ)$ and $100^\circ(280^\circ) \lesssim \delta \lesssim 147^\circ(327^\circ)$ which correspond to the atmospheric mixing angle θ_{23} in the lower octant. Similarly, in Fig. 2a, we use Eqs. (2.28), (2.29), (2.30) along with Eq. (3.2) to indicate the predictions related to the sum of the light neutrino masses against m_1 , the lightest neutrino mass, indicated by the blue patch. The region between the black dotted lines represents 3σ allowed range for $\sum_i m_i$ and the blue patch within it represents the predicted region in our framework. The red shaded region with $\sum_i m_i \leq 0.11$ eV is disallowed by cosmological observation mentioned earlier. This plot shows that the lightest neutrino mass is $\mathcal{O}(10^{-3})$ eV whereas the sum of the light neutrino masses is around $\mathcal{O}(0.06)$ eV. On top of this, the present set up excludes the possibility of having maximum CP violation ($\delta = 90^\circ/270^\circ$) and at the same time

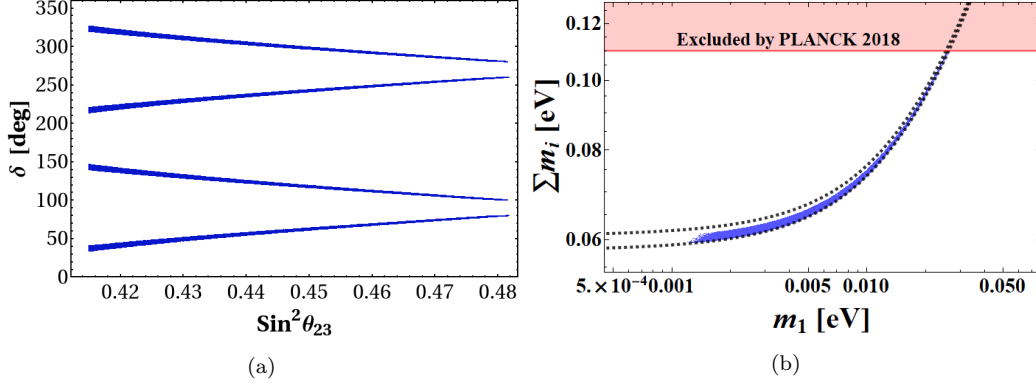


Figure 2: Correlations within $\delta - \theta_{23}$ (left panel) and $\sum_i m_i - m_1$ (right panel) are presented while allowed ranges for χ_1 , χ_2 , γ_1 and γ_2 are used from Fig. 1.

favors θ_{23} to be below maximal mixing, *i.e.* $\theta_{23} < 45^\circ$. These are the salient features of our proposal.

3.3 Neutrinoless Double beta decay

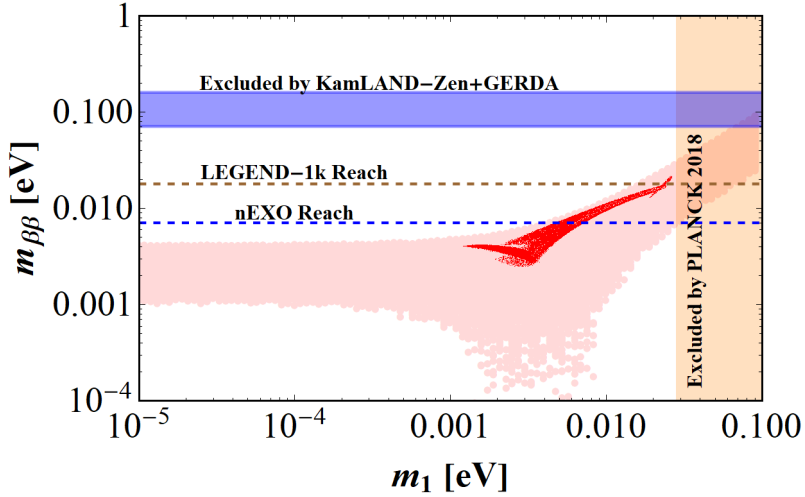


Figure 3: Correlation between $m_{\beta\beta}$ and lightest neutrino mass m_1 (for NH) with allowed ranges for χ_1 , χ_2 , γ_1 and γ_2 obtained from Fig. 1. Here the light blue shaded region represents the combined upper limit of GERDA and KamLAND-Zen experiments whereas the brown and blue dashed lines stand for future sensitivities of the LEGEND and nEXO experiments respectively.

It is pertinent to also shed light on the effective neutrino mass parameter, $m_{\beta\beta}$, involved in the half life of neutrinoless double beta decay in our set-up, which is given by [63]

$$m_{\beta\beta} = |m_1 c_{12}^2 c_{13}^2 + m_2 s_{12}^2 c_{13}^2 e^{i\alpha_{21}} + m_3 s_{13}^2 e^{i(\alpha_{31} - 2\delta)}|. \quad (3.3)$$

Note that for the normal hierarchy of light neutrino masses, one can write $m_2 = \sqrt{(m_1^2 + \Delta m_{21}^2)}$, and $m_3 = \sqrt{(m_1^2 + \Delta m_{31}^2)}$. Recall also that we have already elaborated on our finding for lightest neutrino masses m_1 (see Fig. 2b), and δ (see Fig. 2a) in the last subsections corresponding to the allowed parameter space of $\{\chi_1, \chi_2, \gamma_1, \gamma_2\}$ from Fig. 1. Using the same, we could also estimate the respective allowed ranges of Majorana phases α_{21} and α_{31} via Eq. (2.36) (as $\alpha_{21} = \beta_{21}$ and $\alpha_{31} = \beta_{31}$) and in turn we can evaluate $m_{\beta\beta}$ as function of m_1 (substituting m_2 and m_3 in Eq. (3.3)). With the allowed ranges for χ_1, χ_2, γ_1 and γ_2 satisfying all the neutrino data inclusive of the cosmological mass bounds (*i.e.* corresponding to the dark blue patch of left panel, and four cornered patches of right panel of Fig. 1), we therefore plot $m_{\beta\beta}$ as a function of lightest neutrino masses m_1 for normal hierarchy as presented in Fig. 3 by the red patch. The background light red patch indicates the allowed region in general when mixing angles, mass squared differences along with δ are allowed to vary within their 3σ range. Hence from this $m_{\beta\beta}$ vs m_1 plot (red patch), we notice that for m_1 within the range (0.001-0.027) eV (allowed in our set-up as per Fig. 2b), the effective mass parameter is predicted to be: $0.002 \lesssim m_{\beta\beta} \lesssim 0.021$ eV. This prediction lies well within the limits on $m_{\beta\beta}$ by combined analysis of GERDA and KamLAND-Zen experiments denoted by the light blue shade. The horizontal brown and blue dashed lines stand for future sensitivity by the LEGEND and nEXO experiments.

3.4 Lepton flavor violation

Due to the existence of active-sterile neutrino mixing, the possibility of rare lepton flavor violating processes should arise in our framework. Out of all the processes, contribution to $\mu \rightarrow e\gamma$ is the most important one as it is significantly constrained. In the weak basis, *i.e.* where charged and RHN mass matrix is diagonal, the branching ratio of the same process can be written as [68, 69]:

$$B(\mu \rightarrow e\gamma) = \frac{3\alpha}{8\pi} \left| \sum_i \mathbb{R}_{ei} \mathbb{R}_{i\mu}^\dagger \mathbb{F}\left(\frac{M_i^2}{M_W^2}\right) \right|^2, \quad (3.4)$$

where $\alpha = e^2/4\pi$ is the fine structure constant, M_W stands for W^\pm mass, $\mathbb{R} = m_D M_R^{-1}$ is the mixing matrix representing active-sterile mixing, M_i is the mass of RHN mass eigenstates N_i and $\mathbb{F}(x) = \frac{x(1-6x+3x^2+2x^3-6x^2 \ln x)}{2(1-x)^4}$, with $x = M_i/M_W$. The current upper bound on the branching ratio of the $\mu \rightarrow e\gamma$ is found to be $\text{BR}(\mu \rightarrow e\gamma) \lesssim 4.2 \times 10^{-13}$ (at 90% C.L.) [63]. In our analysis, with the allowed ranges for χ_1, χ_2, γ_1 and γ_2 (obtained from Fig. 1) and M_i in the TeV scale, the contribution towards the branching ratio for $\mu \rightarrow e\gamma$ turns out to be insignificant ($\mathcal{O}(10^{-35})$) compared to the experimental limit.

4 Leptogenesis

The presence of RHNs in the seesaw realization of light neutrino mass provides an opportunity to study leptogenesis from the CP-violating out-of-equilibrium decay of RHNs into lepton and Higgs doublets in the early universe [45, 49, 70]. The lepton asymmetry created

is expected to be converted to a baryon asymmetry via the sphaleron process[71, 72]. In the previous part of our analysis, we have found that the phenomenology of the neutrino sector is mainly dictated by four parameters *i.e* χ_1, χ_2, γ_1 , and γ_2 which in turn determine most of the observables in the neutrino sector. However we also notice the presence of the prefactor $|f_3^\nu|^2 v^2/M$ associated to the light neutrino mass eigenvalues as given in Eq. (2.28)-(2.30). Using Eq. (3.2), though this prefactor can be evaluated, we can't have specific estimate for the degenerate mass of the RHNs (M) as f_3^ν remains undetermined. To have a more concrete picture, we provide a plot for $|f_3^\nu|^2 v^2/M$ against one of the parameters, χ_1 , in Fig. 4 obtained using the correlation with other parameters fixed by neutrino oscillation and cosmological data. Hence barring the ambiguity in determining f_3^ν apart from a conservative limit $|f_3^\nu| < \mathcal{O}(1)$, M is seen to be anywhere from a very large value (say 10^{14-15} GeV) to a low one (say TeV). Furthermore, the RHNs are exactly degenerate

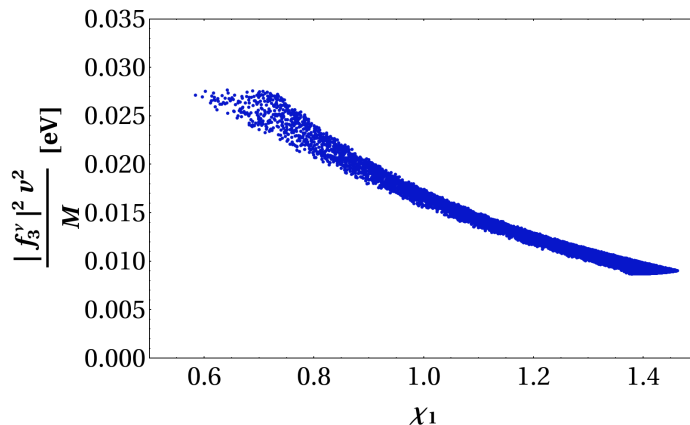


Figure 4: Correlation between $\frac{|f_3^\nu|^2 v^2}{M}$ and χ_1 for NH.

in our framework. Hence unless we break this exact degeneracy, no CP asymmetry can be generated [58]. Below we proceed to discuss leptogenesis mechanism in the present framework keeping in mind that we need to remove the exact degeneracy of RHN masses and study of flavored leptogenesis becomes essential (as M can be below 10^{12} GeV).

4.1 Generation of mass splitting and CP asymmetry

The CP asymmetry parameter generated as a result of the interference between the tree and one loop level decay amplitudes of RHN N_i decaying into a lepton doublet with specific flavor l_α and Higgs (H) is defined by :

$$\epsilon_i^\alpha = \frac{\Gamma(N_i \rightarrow \ell_\alpha H) - \Gamma(N_i \rightarrow \bar{\ell}_\alpha \bar{H})}{\Gamma(N_i \rightarrow \ell_\alpha H) + \Gamma(N_i \rightarrow \bar{\ell}_\alpha \bar{H})}. \quad (4.1)$$

Considering the exact mass degeneracy is lifted by some mechanism (will be discussed soon), the general expression for such asymmetry can be written as [73, 74] :

$$\begin{aligned} \epsilon_i^\alpha = & \frac{1}{8\pi\mathcal{H}_{ii}} \sum_{j \neq i} \text{Im}[\mathcal{H}_{ij}(\mathcal{Y}^{\nu\dagger})_{i\alpha}(\mathcal{Y}^\nu)_{\alpha j}] \left[f(x_{ij}) + \frac{\sqrt{x_{ij}}(1-x_{ij})}{(1-x_{ij})^2 + \frac{\mathcal{H}_{jj}^2}{64\pi^2}} \right] \\ & + \frac{1}{8\pi\mathcal{H}_{ii}} \sum_{j \neq i} \text{Im}[\mathcal{H}_{ji}(\mathcal{Y}^{\nu\dagger})_{i\alpha}(\mathcal{Y}^\nu)_{\alpha j}] \left[\frac{(1-x_{ij})}{(1-x_{ij})^2 + \frac{\mathcal{H}_{jj}^2}{64\pi^2}} \right], \end{aligned} \quad (4.2)$$

where \mathcal{Y}^ν ($\equiv V^\dagger Y^\nu$ in our case, see Eq. (2.11)) is the neutrino Yukawa matrix in charge lepton diagonal basis, \mathcal{H} and the loop factor $f(x_{ij})$ are given by

$$\mathcal{H} = \mathcal{Y}^{\nu\dagger} \mathcal{Y}^\nu = Y^{\nu\dagger} Y^\nu; \quad (4.3)$$

$$f(x_{ij}) = \sqrt{x_{ij}} \left[1 - (1+x_{ij}) \ln \left(\frac{1+x_{ij}}{x_{ij}} \right) \right], \quad (4.4)$$

with $x_{ij} = \frac{M_j^2}{M_i^2}$ where M_i are the masses of the RHNs after the degeneracy is removed. This is applicable for both hierarchical as well as quasi-degenerate mass spectrum of RHNs [73]. For the hierarchical RHNs, one neglects $\frac{\mathcal{H}_{jj}^2}{64\pi^2}$ compared to $(1-x_{ij})^2$ while the entire expression of Eq. (4.2) can be used for quasi-degenerate case inclusive of resonance situation for which $(1-x_{ij})^2 \simeq \frac{\mathcal{H}_{jj}^2}{64\pi^2}$ [74, 75]. Below we discuss the mass splittings induced by the running of the heavy RHNs.

4.1.1 Lifting the mass degeneracy

The exact mass degeneracy of heavy Majorana neutrinos is the result of the flavor symmetry imposed in our construction. To remove this degeneracy, here we adopt the renormalization group effects into consideration [76, 77]. Considering the discrete $A_4 \times Z_3 \times Z_2$ symmetry breaking scale close to the GUT scale $\sim \Lambda$ (the cut-off scale introduced in Eq. (2.1)), we determine the running of the RHN mass matrix M_R and Dirac neutrino Yukawa matrix \mathcal{Y}^ν from GUT scale to seesaw scale M (assuming $M < \Lambda$). Using renormalisation group equations, the evolution of the RHN mass matrix M ($= \text{diag}(M_1, M_2, M_3)$) and Dirac neutrino Yukawa matrix \mathcal{Y}^ν (in charged lepton Y^ℓ diagonal basis) at one-loop can be written as [76–78]

$$\frac{dM_i}{dt} = 2M_i \mathcal{H}_{ii}, \quad (4.5)$$

$$\frac{d\mathcal{Y}^\nu}{dt} = \left[\left\{ \mathcal{T} - \frac{3}{4}g_1^2 - \frac{9}{4}g_2^2 \right\} \mathbb{I}_3 - \frac{3}{2} \left(Y^\ell Y^{\ell\dagger} - \mathcal{Y}^\nu \mathcal{Y}^{\nu\dagger} \right) \right] \mathcal{Y}^\nu + \mathcal{Y}^\nu R, \quad (4.6)$$

with

$$\mathcal{T} = 3\text{Tr}(Y_u Y_u^\dagger) + 3\text{Tr}(Y_d Y_d^\dagger) + \text{Tr}(Y^\ell Y^{\ell\dagger}) + \text{Tr}(\mathcal{Y}^\nu \mathcal{Y}^{\nu\dagger}), \quad (4.7)$$

where $Y_{u,d}$ are the up-quark and down-quark Yukawa matrices respectively, $g_{1,2}$ are the gauge couplings and \mathbb{I}_3 is the identity matrix of order 3×3 . Here the matrix R is anti-

hermitian defined by [77]

$$\begin{aligned} R_{11} &= R_{22} = R_{33} = 0, \quad R_{ji} = -R_{ij}^* (i \neq j), \\ R_{ij} &= \frac{2 + \delta_{ij}}{\delta_{ij}} \operatorname{Re}(\mathcal{H}_{ij}) + i \frac{\delta_{ij}}{2 + \delta_{ij}} \operatorname{Im}(\mathcal{H}_{ij}), \end{aligned} \quad (4.8)$$

$\delta_{ij} = \frac{M_j}{M_i} - 1$ is the degeneracy parameter for the RHN masses and $t = \frac{1}{16\pi^2} \ln\left(\frac{\Lambda}{M}\right)$.

Now as the RHNs are exactly degenerate at scale Λ , the right hand side (first term) of Eq. (4.8) becomes singular unless we impose $\operatorname{Re}(\mathcal{H}_{ij}) = 0$. Note that, in our construction, \mathcal{H}_{12} and \mathcal{H}_{23} are already zero due to the flavor symmetry imposed. Hence the above condition should be exercised only to realize $\operatorname{Re}(\mathcal{H}_{13}) = 0$ in our case which can be materialized if we choose to use $\tilde{\mathcal{Y}}^\nu$, obtained by performing an orthogonal rotation (by a matrix O say) on Dirac Yukawa matrix \mathcal{Y}^ν as,

$$\tilde{\mathcal{Y}}^\nu = \mathcal{Y}^\nu O, \quad \text{with} \quad O = \begin{pmatrix} \cos \Theta & 0 & \sin \Theta \\ 0 & 1 & 0 \\ -\sin \Theta & 0 & \cos \Theta \end{pmatrix}, \quad (4.9)$$

having the rotation angle Θ determined by the relation

$$\tan 2\Theta = \frac{2\operatorname{Re}(\mathcal{H}_{13})}{\mathcal{H}_{33} - \mathcal{H}_{11}} = \frac{-\cos \gamma_1}{\chi_2 \cos(\gamma_1 - \gamma_2)}. \quad (4.10)$$

In obtaining the rightmost expression above, we employ Eqs. (2.6), (2.22), (2.23) in Eq. (4.3). This flexibility in using $\tilde{\mathcal{Y}}^\nu$ prevails due the following reason. Note that, if we rotate the \mathcal{Y}^ν in this manner, the neutrino Yukawa Lagrangian gets modified to:

$$\bar{\ell}_L \mathcal{Y}^\nu \tilde{H} N_R = \bar{\ell}_L \tilde{\mathcal{Y}}^\nu O^T \tilde{H} N_R. \quad (4.11)$$

We can now redefine N_R by: $\tilde{N}_R = O^T N_R$, *i.e.* if we rotate RHN fields by O^T , RHN mass term will not change as $\bar{N}_R^C M_R N_R = \tilde{N}_R^C M_R \tilde{N}_R$ due to the orthogonal property of O matrix.

The Eqs. (4.5) and (4.6) can now be rewritten in terms of $\tilde{\mathcal{H}} = O^T \mathcal{H} O$ and $\tilde{\mathcal{Y}}^\nu$ by using the above relations. The form of $\tilde{\mathcal{H}}$ can be obtained by

$$\tilde{\mathcal{H}} = \tilde{\mathcal{Y}}^{\nu\dagger} \tilde{\mathcal{Y}}^\nu = O^T \mathcal{H} O = \begin{pmatrix} \mathcal{H}_{11} - \Delta & 0 & i \operatorname{Im}(\mathcal{H}_{13}) \\ 0 & \mathcal{H}_{22} & 0 \\ -i \operatorname{Im}(\mathcal{H}_{13}) & 0 & \mathcal{H}_{33} + \Delta \end{pmatrix}, \quad (4.12)$$

where $\Delta \equiv \tan \Theta \operatorname{Re}(\mathcal{H}_{13})$. As seen from the Eq. (4.5) (with right hand side written in terms of $\tilde{\mathcal{H}}$ now), we find that a mass splitting generated at a scale (M) as

$$\delta_{ij}^M = 2(\tilde{\mathcal{H}}_{ii} - \tilde{\mathcal{H}}_{jj})t, \quad (4.13)$$

thanks to the effect of running. Using Eq. (4.6), we also get a off-diagonal contribution ($\mathcal{H}_{ij}^R, i \neq j$) to $\tilde{\mathcal{H}}$ [77],

$$\tilde{\mathcal{H}}_{ij}^M = \tilde{\mathcal{H}}_{ij} + \mathcal{H}_{ij}^R; \quad \mathcal{H}_{ij}^R \simeq 3y_\tau^2 \tilde{\mathcal{Y}}_{3i}^{\nu*} \tilde{\mathcal{Y}}_{3j}^\nu t; \quad (i \neq j) \quad (4.14)$$

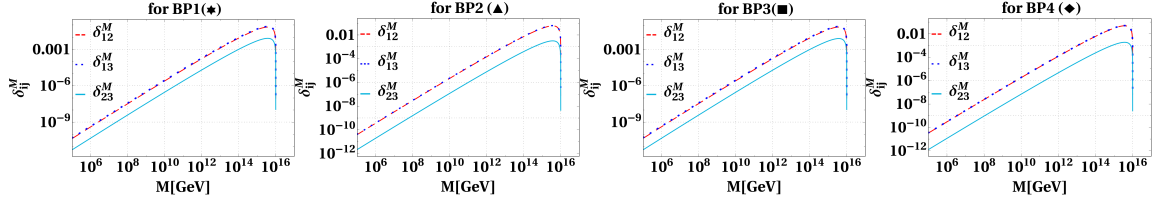


Figure 5: Variation of mass splitting δ_{ij}^M with respect to scale M for the benchmark points BP1, BP2, BP3 and BP4 respectively.

while $\tilde{\mathcal{H}}_{ii}^M = \tilde{\mathcal{H}}_{ii}$. As mentioned earlier, the seesaw scale M remains undetermined even after applying neutrino mass and mixing constraints, we have shown in Fig. 5 how such splitting δ_{12}^M varies with the degenerate RHN mass M due to running corresponding to benchmark points: BP1, BP2, BP3 and BP4 allowed by the neutrino data. We find that below $M \simeq 10^{12}$ GeV, δ_{ij}^M become smaller than $\mathcal{O}(10^{-4})$ implying that the masses of the three RHNs fall in the quasi-degenerate category [73]. Such a small splitting, although crucial for generation of CP asymmetry, won't alter our findings of the neutrino section. Note that the estimated splitting does not correspond to the requirement of resonant leptogenesis. We are now in a position to evaluate the CP asymmetry generated at scale M , as discussed below.

4.1.2 Estimating CP asymmetry

Starting with exact degeneracy of RHN masses, we have shown that the running of involved parameters from a typical high scale to the scale of the heavy neutrino masses leads to a quasi-degenerate spectrum of RHNs. Hence we can now estimate the CP asymmetry created at a scale M by using Eq. (4.2) while replacing \mathcal{H} by $\tilde{\mathcal{H}}^M$ and δ_{ij} by δ_{ij}^M in view of our discussion above. Furthermore, it can be shown that maximum contribution to CP asymmetry comes from self energy diagram [48, 79, 80]. Therefore, the asymmetry expression of Eq. (4.2) gets modified to

$$\epsilon_i^\alpha \simeq -\frac{1}{16\pi\tilde{\mathcal{H}}_{ii}^M} \sum_{j \neq i} \frac{\delta_{ij}^M}{(\delta_{ij}^M)^2 + \left(\frac{\tilde{\mathcal{H}}_{jj}^M}{16\pi}\right)^2} \left\{ \text{Im}[\tilde{\mathcal{H}}_{ij}^M \tilde{\mathcal{Y}}_{\alpha i}^{\nu*} \tilde{\mathcal{Y}}_{\alpha j}^\nu] + \text{Im}[\tilde{\mathcal{H}}_{ji}^M \tilde{\mathcal{Y}}_{\alpha i}^{\nu*} \tilde{\mathcal{Y}}_{\alpha j}^\nu] \right\}. \quad (4.15)$$

Now, using Eqs. (4.12) to (4.14) and employing them in Eq. (4.15), we estimate for the cp asymmetry parameter for the heavy RHNs decaying into various flavors which will be useful to evaluate the final lepton asymmetry taking the flavor effects into account. Since all the entities of Eq. (4.15) are function of set of parameters $\{\chi_1, \chi_2, \gamma_1, \gamma_2\}$ and M , we can make use of the allowed parameter space from neutrino phenomenology (refer to Fig. 1) and finally calculate the CP asymmetries produced from all three RHN decays ($i = 1, 2, 3$) to different flavors of lepton doublets and Higgs.

For representation purpose, in Fig. 6, we depict the variation of individual flavor components of CP asymmetry with respect to χ_1 at three different RHN mass scales: $M =$

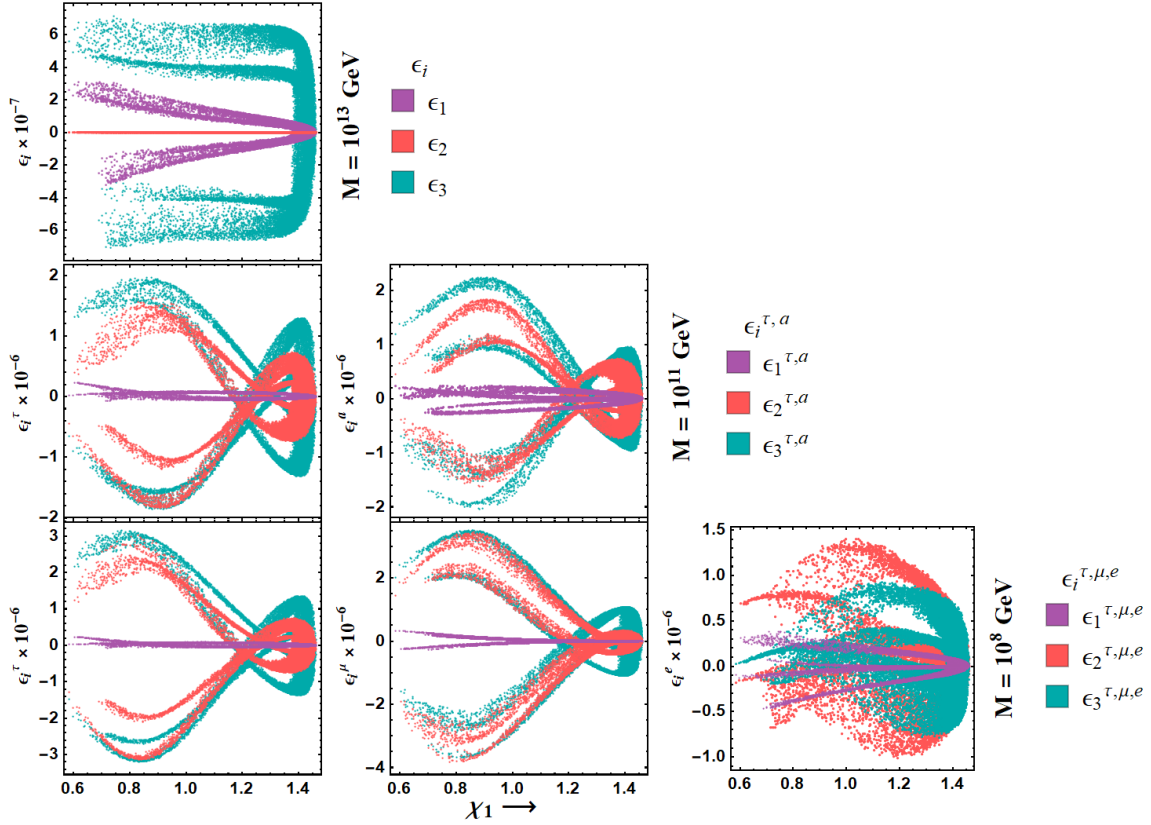


Figure 6: Variation of individual components of CP asymmetry with respect to model parameter χ_1 for three different scales $M = 10^{13}$ GeV (top most plot), $M = 10^{11}$ GeV (plots from second row) and $M = 10^8$ GeV (plots from third row).

10^{13} (top panel), 10^{11} (middle panel), 10^8 (bottom panel) GeV respectively. Since the flavor effects are known not to be important beyond $T \sim M \simeq 10^{12}$ GeV, we estimate asymmetries produced by individual RHNs only for top panel. It is found that maximum asymmetry falls in the ballpark of $|\epsilon_{i=1,3}|_{\max} \sim 6 \times 10^{-7}$ whereas $(|\epsilon_2|)_{\max}$ remains subdominant. At $T = 10^{11}$ GeV (and above 10^8 GeV), tau Yukawa comes to equilibrium, so effectively the scenario with $M = 10^{11}$ GeV becomes a two flavor scenario (τ and another orthogonal direction, say a) and the corresponding CP asymmetries are marked by: $\{\epsilon_i^\tau, \epsilon_i^{a=\mu+e}\}$. At this scale, $|\epsilon_{i=2,3}^{\tau,a}|_{\max} \sim 2 \times 10^{-6}$ (middle panel of Fig. 6) and $|\epsilon_1^{\tau,a}|_{\max}$ becomes relatively small. We also estimate CP asymmetry at $M = 10^8$ GeV (bottom panel of Fig. 6). At this temperature (or scale), all Yukawa couplings are in equilibrium and hence contributions to CP asymmetries from all the three flavors, $\{\epsilon_i^e, \epsilon_i^\mu, \epsilon_i^\tau\}$, become important. We find $|\epsilon_{i=2,3}^{\tau}|_{\max} \sim 3 \times 10^{-6}$ and $|\epsilon_1^\tau|_{\max} < |\epsilon_{i=2,3}^{\tau}|_{\max}$. An analogous pattern is observed for ϵ_i^μ . CP asymmetry along electron flavor is shown in the third plot of the bottom panel of Fig. 6 and is found to be $|\epsilon_{i=2,3}^e|_{\max} \sim 1.5 \times 10^{-6}$, $|\epsilon_1^e|_{\max} \sim 5 \times 10^{-7}$. With these various flavor dependent CP asymmetries, we can now proceed for evaluation of baryon asymmetry by solving the Boltzmann equations as illustrated below.

4.2 Solution of Boltzmann equation

It is worth mentioning that while estimating the final lepton asymmetry, one needs to take care of decays and inverse decays of heavy RHNs as well as various scattering processes. As stated earlier, we consider the contributions of all three RHNs having $M_i \lesssim 10^{12}$ GeV. Hence flavor effects have to be considered [81] as with the mass equivalent temperature regime $T \sim 10^{12}$ GeV, decay rate of τ ($\Gamma_\tau \sim 5 \times 10^{-3} y_\tau^2 T$) [82, 83] becomes comparable to the Hubble expansion rate. Below this temperature, the relation becomes $\Gamma_\tau > H$ indicative of the start of equilibrium era for τ Yukawa interactions and τ lepton doublet becomes distinguishable. In a similar way, for the temperature regime $10^8 \text{ GeV} \lesssim T \lesssim 10^{11} \text{ GeV}$, muon Yukawa interaction comes to equilibrium (and both μ and τ flavors of lepton doublets are distinguishable henceforth) and finally below $T \lesssim 10^8 \text{ GeV}$, e Yukawa interaction are in equilibrium.

In our analysis, therefore, we include these flavor effects into consideration while constructing the Boltzmann equations. We work in a most general setup for leptogenesis, where all three RHNs are contributing to the asymmetry due to their quasi degenerate spectrum of masses. As standard, the produced lepton doublets from the RHN decay needs to be appropriately projected to flavor states in the three above mentioned temperature regimes differently where the related respective lepton asymmetries are characterized by the C^ℓ matrices (C^H stands for that of Higgs) [84, 85]. For example, when only the τ Yukawa interaction is in equilibrium ($10^{11} \text{ GeV} \lesssim T \lesssim 10^{13} \text{ GeV}$), effectively the scenario becomes a two flavor case (as the flavor space is spanned by ℓ_τ and another orthogonal direction) and so C^ℓ is a matrix of order 2×2 . For a further smaller temperature, the situation comprises of three effective flavors and so C^ℓ is of 3×3 . Below we write down the relevant Boltzmann equations to study the time evolution of the lepton-number asymmetries (for a system of three RHNs) as [84–86]

$$sH z \frac{dY_{N_i}}{dz} = - \left\{ \left(\frac{Y_{N_i}}{Y_{N_i}^{\text{eq}}} - 1 \right) (\gamma_{D_i} + 2\gamma_{N_s^i} + 4\gamma_{N_t^i}) + \sum_{j \neq i} \left(\frac{Y_{N_i}}{Y_{N_i}^{\text{eq}}} \frac{Y_{N_j}}{Y_{N_j}^{\text{eq}}} - 1 \right) (\gamma_{N_i N_j}^{(1)} + \gamma_{N_i N_j}^{(2)}) \right\}, \quad (4.16)$$

$$\begin{aligned} sH z \frac{dY_{\Delta_\alpha}}{dz} = & - \left\{ \sum_i \left(\frac{Y_{N_i}}{Y_{N_i}^{\text{eq}}} - 1 \right) \epsilon_i^\alpha \gamma_{D_i} - \sum_\beta \left[\sum_i \left(\frac{1}{2} (C_{\alpha\beta}^\ell - C_\beta^H) \right) \gamma_{D_i}^\alpha \right. \right. \\ & + \left(C_{\alpha\beta}^\ell \frac{Y_{N_i}}{Y_{N_i}^{\text{eq}}} - \frac{C_\beta^H}{2} \right) \gamma_{N_s^i} + \left(2C_{\alpha\beta}^\ell - \frac{C_\beta^H}{2} \left(1 + \frac{Y_{N_i}}{Y_{N_i}^{\text{eq}}} \right) \right) \gamma_{N_t^i} \\ & \left. \left. + \sum_\gamma \left((C_{\alpha\beta}^\ell + C_{\gamma\beta}^\ell - 2C_\beta^H) (\gamma_N^{(1)\alpha\gamma} + \gamma_N^{(2)\alpha\gamma}) \sum_{i,j} (C_{\alpha\beta}^\ell - C_{\gamma\beta}^\ell) \gamma_{N_i N_j}^{(1)\alpha\gamma} \right) \right] \frac{Y_{\Delta_\beta}}{Y^{\text{eq}}} \right\}, \quad (4.17) \end{aligned}$$

where $z = M_i/T$ and $\alpha = e, \mu, \tau$. In the above, $Y_{\Delta_\alpha(N_i)} = n_{\Delta_\alpha(N_i)}/s$ denotes the density of $\Delta_\alpha = \frac{B}{3} - L_\alpha$ (relevant heavy neutrino) with respect to the entropy s , Y^{eq} 's are the

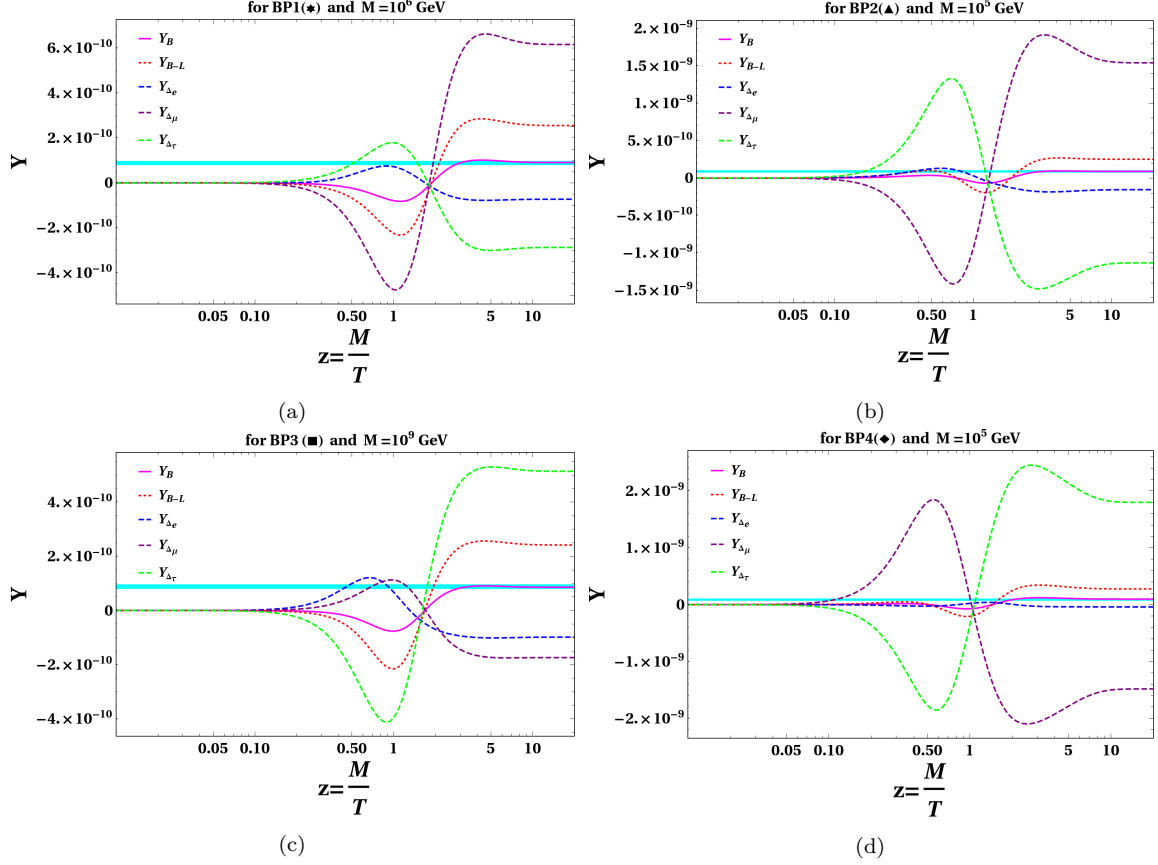


Figure 7: Variation of Y_B , Y_{B-L} , Y_{Δ_e} , Y_{Δ_μ} , Y_{Δ_τ} (denoted by solid magenta, dotted red, dashed blue, dashed pink and dashed green lines respectively) presented as function of $z = M/T$. Here we have considered one benchmark point from each of the four patches of γ_2 vs γ_1 plot for the light neutrino parameters of the model (from Fig. 1).

respective number densities while in thermal equilibrium. Here, total decay rate density of N_i is given by

$$\gamma_{D_i} = \sum_{\alpha} [\gamma(N_i \rightarrow \ell_{\alpha} + H) + \gamma(N_i \rightarrow \bar{\ell}_{\alpha} + \bar{H})] = n_{N_i}^{eq} \frac{K_1(z)}{K_2(z)} \Gamma_i, \quad (4.18)$$

where Γ_i is the total decay rate of N_i at tree level and written as

$$\Gamma_i = \sum_{\alpha} [\Gamma(N_i \rightarrow \ell_{\alpha} + H) + \Gamma(N_i \rightarrow \bar{\ell}_{\alpha} + \bar{H})], \quad (4.19)$$

and $\gamma_{N_s^i}, \gamma_{N_t^i}$ (both are Higgs mediated scattering process with change in lepton number $\Delta L = 1$), $\gamma_{N_i N_j}^{(1)}, \gamma_{N_i N_j}^{(2)}$ (both are neutrino pair annihilation process) are the reaction rate densities for the scattering processes: $[N_i + \ell \leftrightarrow Q + \bar{U}]_s$, $[N_i + \bar{Q} \leftrightarrow \bar{\ell} + \bar{U}]_t$ and $[N_i + U \leftrightarrow \bar{\ell} + \bar{Q}]_t$, $[N_i + N_j \leftrightarrow \ell + \bar{\ell}]$ and $[N_i + N_j \leftrightarrow H + \bar{H}]$ respectively [47, 87]. Here in Eq. (4.18), $K_1(z)$ and $K_2(z)$ are the modified Bessel functions.

With all the ingredients at hand, we first substitute the evaluated CP asymmetry (from Eq. (4.15)) in Eq. (4.17) and proceed for solving the coupled Boltzmann equations

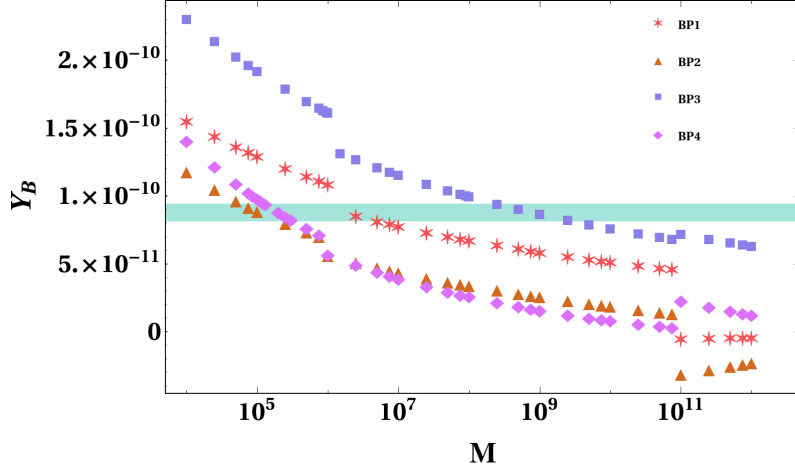


Figure 8: Variation of final Y_B with respect to M (neglecting $\Delta L = 2$ processes) for four benchmark point BP1, BP2, BP3, BP4, from each of the four patches of γ_2 vs γ_1 plot for the light neutrino parameters of the model (from Fig. 1). Here the horizontal patch (light greenish-blue) indicates the observed value of baryon asymmetry [67].

in order to find out the final lepton asymmetry as well as final baryon asymmetry. In doing so, we divide the temperature range into three zones so as to take care of the flavor effects as discussed before while taking into account the $\Delta L = 1$ processes (and ignoring $\Delta L = 2$ processes). We have considered different benchmark values for RHN degenerate mass M (splittings are automatically taken care of by running in terms of other parameters): $M = 10^9, 10^6, 10^5$ GeV so that the effects of flavor can be visible. These benchmark values of M are so chosen that they can produce requisite amount of baryon asymmetry corresponding to a specific choice of parameters: $\{\chi_1, \chi_2, \gamma_1, \gamma_2\}$.

In Fig. 7, we present our findings in terms of estimate of the evolution of the $B - L$ asymmetry (denoted by red dotted line) as well as B asymmetry (denoted by Magenta solid line) for specific choices of the parameters $\{\chi_1, \chi_2, \gamma_1, \gamma_2\}$ which correctly produce neutrino data as discussed in Section 3. Fig. 7a, 7b, 7c, 7d represent the benchmark points BP1, BP2, BP3, and BP4 respectively from the allowed cornered patches of γ_1 and γ_2 plot of Fig. 1. Asymmetries of individual flavors are also drawn in these figures.

While solving the Boltzmann equations, we have assumed that initially the abundance of all the RHNs was very less and they were out of equilibrium. Then due to annihilation of bath particles it gets produced and comes to equilibrium. Around $\frac{M}{T} \sim 1$, the production rate and decay rate of the RHN become almost equal and afterward the decay rate dominates over the production rate and hence it's abundance starts to fall. The correct baryon asymmetry can be produced with $M \lesssim 10^6$ GeV for BP1, $M \lesssim 10^5$ GeV for BP2 and BP4, $M \lesssim 10^9$ GeV for BP3 region respectively. For these individual sets of parameters, we have checked the variation of final baryon asymmetry, Y_B , with respect to mass of M as shown in Fig. 8. From this Fig. 8, we also see that final Y_B is increasing with the decreasing of M . There seems to be two discontinuities for each such plot. For example, with blue-dotted line, these are observed at or around $M = 10^{11}$ GeV and at $M = 10^6$

GeV. These are indicative of the eras where different flavors of lepton doublets enter in (or exit from) equilibrium and the Boltzmann equations get modified.

5 Conclusion

In this analysis, we present an economical, predictive flavor symmetric setup based on $A_4 \times Z_3 \times Z_2$ discrete group to explain neutrino masses, mixing via type-I seesaw mechanism while matter-antimatter asymmetry is also addressed via leptogenesis. In the original AF model, TBM mixing scheme was realized introducing three flavon fields. With similar fields content, here we show that correct neutrino mixing and mass-squared differences are originated from non-trivial structure of the neutrino Dirac Yukawa coupling and diagonal RHN mass matrix, thanks to the contribution from the charged lepton sector too. In particular, the antisymmetric contribution in the Dirac Yukawa coupling plays an instrumental role in generating the non-zero θ_{13} . Using the current experimental observation on neutrino oscillation and other cosmological limits, we find the allowed parameter space for parameters $\chi_1, \chi_2, \gamma_1, \gamma_2$ which in turn not only restricts some of the observables associated to neutrinos like Dirac CP phase, neutrino-less double beta decay, lepton flavor violating decays, estimation of Majorana phases etc. but also are helpful in determining the matter-antimatter asymmetry of the universe. More specifically, we find that this model is highly predictive in nature. Only normal mass hierarchies are found to be allowed in the current setup. Interestingly the atmospheric mixing angle θ_{23} lies in the lower octant while the leptonic Dirac CP phase falls within the range $33^\circ(213^\circ) \lesssim \delta \lesssim 80^\circ(260^\circ)$ and $100^\circ(280^\circ) \lesssim \delta \lesssim 147^\circ(327^\circ)$. Apart from these predictions for absolute neutrino mass and effective mass parameter appearing the neutrino-less double beta decay have also been made. The model also predicts an interesting correlation between the atmospheric mixing angle θ_{23} and the Dirac CP phase which is a feature of the specific flavor symmetry considered here. At high scale, owing to the symmetry of the model, the heavy RHNs are found to be exactly degenerate apparently forbidding the generation of baryon asymmetry via leptogenesis. However, this is accomplished here elegantly by considering the renormalization group effects into the picture. A tiny mass splitting produced as a result of running from a high scale (GUT scale) to the scale of RHN mass opens the room for leptogenesis. We have incorporated the flavor effects in leptogenesis as our working regime of RHN mass falls near or below 10^9 GeV. Finally, we figure out that the parameter space allowed by the neutrino data in fact is good enough to generate sufficient amount of baryon asymmetry of the universe with RHN mass as low as 10^5 GeV.

Acknowledgements

The work by BK is supported by the Polish National Science Centre (NCN) under the Grant Agreement 2020/37/B/ST2/02371 and DST, Govt. of India (SR/MF/PS-01/2016-IITH/G). BK also acknowledges the support provided by the Institute of High Energy Physics and the University of Chinese Academy of Sciences, Beijing, China, where part

of the work has been completed. AD would like to thank Rishav Roshan and Dibyendu Nanda for fruitful discussions.

Appendix

A A_4 Multiplication Rules:

It has four irreducible representations: three one-dimensional and one three dimensional which are denoted by $\mathbf{1}$, $\mathbf{1}'$, $\mathbf{1}''$ and $\mathbf{3}$ respectively. The multiplication rules of the irreducible representations are given by [18]

$$\mathbf{1} \otimes \mathbf{1} = \mathbf{1}, \mathbf{1}' \otimes \mathbf{1}' = \mathbf{1}'', \mathbf{1}'' \otimes \mathbf{1}'' = \mathbf{1}, \mathbf{1}'' \otimes \mathbf{1}' = \mathbf{1}', \mathbf{3} \otimes \mathbf{3} = \mathbf{1} + \mathbf{1}' + \mathbf{1}'' + \mathbf{3}_a + \mathbf{3}_s \quad (\text{A.1})$$

where \mathbf{a} and \mathbf{s} in the subscript corresponds to anti-symmetric and symmetric parts respectively. Now, if we have two triplets as $A = (a_1, a_2, a_3)^T$ and $B = (b_1, b_2, b_3)^T$ respectively, their direct product can be decomposed into the direct sum mentioned above. The product rule for this two triplets in the S diagonal basis⁶ can be written as

$$(A \times B)_1 \sim a_1 b_1 + a_2 b_2 + a_3 b_3, \quad (\text{A.2})$$

$$(A \times B)_{1'} \sim a_1 b_1 + \omega^2 a_2 b_2 + \omega a_3 b_3, \quad (\text{A.3})$$

$$(A \times B)_{1''} \sim a_1 b_1 + \omega a_2 b_2 + \omega^2 a_3 b_3, \quad (\text{A.4})$$

$$(A \times B)_{\mathbf{3}_s} \sim (a_2 b_3 + a_3 b_2, a_3 b_1 + a_1 b_3, a_1 b_2 + a_2 b_1), \quad (\text{A.5})$$

$$(A \times B)_{\mathbf{3}_a} \sim (a_2 b_3 - a_3 b_2, a_3 b_1 - a_1 b_3, a_1 b_2 - a_2 b_1), \quad (\text{A.6})$$

here $\omega (= e^{2i\pi/3})$ is the cube root of unity.

References

- [1] SUPER-KAMIOKANDE collaboration, *Constraints on neutrino oscillations using 1258 days of Super-Kamiokande solar neutrino data*, *Phys. Rev. Lett.* **86** (2001) 5656 [[hep-ex/0103033](#)].
- [2] SUPER-KAMIOKANDE collaboration, *Determination of solar neutrino oscillation parameters using 1496 days of Super-Kamiokande I data*, *Phys. Lett. B* **539** (2002) 179 [[hep-ex/0205075](#)].
- [3] SUPER-KAMIOKANDE collaboration, *A Measurement of atmospheric neutrino oscillation parameters by SUPER-KAMIOKANDE I*, *Phys. Rev. D* **71** (2005) 112005 [[hep-ex/0501064](#)].
- [4] SNO collaboration, *Direct evidence for neutrino flavor transformation from neutral current interactions in the Sudbury Neutrino Observatory*, *Phys. Rev. Lett.* **89** (2002) 011301 [[nucl-ex/0204008](#)].
- [5] SNO collaboration, *Measurement of day and night neutrino energy spectra at SNO and constraints on neutrino mixing parameters*, *Phys. Rev. Lett.* **89** (2002) 011302 [[nucl-ex/0204009](#)].
- [6] KAMLAND collaboration, *Precision Measurement of Neutrino Oscillation Parameters with KamLAND*, *Phys. Rev. Lett.* **100** (2008) 221803 [[0801.4589](#)].

⁶Here S is a 3×3 diagonal generator of A_4 .

- [7] T2K collaboration, *Indication of Electron Neutrino Appearance from an Accelerator-produced Off-axis Muon Neutrino Beam*, *Phys. Rev. Lett.* **107** (2011) 041801 [[1106.2822](#)].
- [8] DOUBLE CHOOZ collaboration, *Indication for the disappearance of reactor electron antineutrinos in the Double Chooz experiment*, *Phys. Rev. Lett.* **108** (2012) 131801 [[1112.6353](#)].
- [9] T2K collaboration, *Observation of Electron Neutrino Appearance in a Muon Neutrino Beam*, *Phys. Rev. Lett.* **112** (2014) 061802 [[1311.4750](#)].
- [10] P. Minkowski, $\mu \rightarrow e\gamma$ at a Rate of One Out of 10^9 Muon Decays?, *Phys. Lett. B* **67** (1977) 421.
- [11] M. Gell-Mann, P. Ramond and R. Slansky, *Complex Spinors and Unified Theories*, *Conf. Proc. C* **790927** (1979) 315 [[1306.4669](#)].
- [12] R.N. Mohapatra and G. Senjanovic, *Neutrino Mass and Spontaneous Parity Violation*, *Phys. Rev. Lett.* **44** (1980) 912.
- [13] R.N. Mohapatra, *Mechanism for Understanding Small Neutrino Mass in Superstring Theories*, *Phys. Rev. Lett.* **56** (1986) 561.
- [14] M. Magg and C. Wetterich, *Neutrino Mass Problem and Gauge Hierarchy*, *Phys. Lett. B* **94** (1980) 61.
- [15] G. Lazarides, Q. Shafi and C. Wetterich, *Proton Lifetime and Fermion Masses in an $SO(10)$ Model*, *Nucl. Phys. B* **181** (1981) 287.
- [16] J. Schechter and J.W.F. Valle, *Neutrino Masses in $SU(2) \times U(1)$ Theories*, *Phys. Rev.* **D22** (1980) 2227.
- [17] R.N. Mohapatra and J.W.F. Valle, *Neutrino Mass and Baryon Number Nonconservation in Superstring Models*, *Phys. Rev. D* **34** (1986) 1642.
- [18] G. Altarelli and F. Feruglio, *Discrete Flavor Symmetries and Models of Neutrino Mixing*, *Rev. Mod. Phys.* **82** (2010) 2701 [[1002.0211](#)].
- [19] Z.-z. Xing, *Flavor structures of charged fermions and massive neutrinos*, *Phys. Rept.* **854** (2020) 1 [[1909.09610](#)].
- [20] S.F. King, *Models of Neutrino Mass, Mixing and CP Violation*, *J. Phys. G* **42** (2015) 123001 [[1510.02091](#)].
- [21] W. Grimus and P.O. Ludl, *Finite flavour groups of fermions*, *J. Phys. A* **45** (2012) 233001 [[1110.6376](#)].
- [22] S.F. King, *Unified Models of Neutrinos, Flavour and CP Violation*, *Prog. Part. Nucl. Phys.* **94** (2017) 217 [[1701.04413](#)].
- [23] S.F. King and C. Luhn, *Trimaximal neutrino mixing from vacuum alignment in A_4 and S_4 models*, *JHEP* **09** (2011) 042 [[1107.5332](#)].
- [24] S.F. King and C. Luhn, *Neutrino Mass and Mixing with Discrete Symmetry*, *Rept. Prog. Phys.* **76** (2013) 056201 [[1301.1340](#)].
- [25] H. Ishimori, T. Kobayashi, H. Ohki, Y. Shimizu, H. Okada and M. Tanimoto, *Non-Abelian Discrete Symmetries in Particle Physics*, *Prog. Theor. Phys. Suppl.* **183** (2010) 1 [[1003.3552](#)].

- [26] D. Wyler, *Discrete Symmetries in the Six Quark $SU(2) \times U(1)$ Model*, *Phys. Rev. D* **19** (1979) 3369.
- [27] G.C. Branco, H.P. Nilles and V. Rittenberg, *Fermion Masses and Hierarchy of Symmetry Breaking*, *Phys. Rev. D* **21** (1980) 3417.
- [28] G. Altarelli and F. Feruglio, *Tri-bimaximal neutrino mixing, $A(4)$ and the modular symmetry*, *Nucl. Phys. B* **741** (2006) 215 [[hep-ph/0512103](#)].
- [29] G. Altarelli and F. Feruglio, *Tri-bimaximal neutrino mixing from discrete symmetry in extra dimensions*, *Nucl. Phys. B* **720** (2005) 64 [[hep-ph/0504165](#)].
- [30] E. Ma and G. Rajasekaran, *Softly broken $A(4)$ symmetry for nearly degenerate neutrino masses*, *Phys. Rev. D* **64** (2001) 113012 [[hep-ph/0106291](#)].
- [31] E. Ma, *$A(4)$ symmetry and neutrinos with very different masses*, *Phys. Rev. D* **70** (2004) 031901 [[hep-ph/0404199](#)].
- [32] G. Altarelli and D. Meloni, *A Simplest A_4 Model for Tri-Bimaximal Neutrino Mixing*, *J. Phys. G* **36** (2009) 085005 [[0905.0620](#)].
- [33] P.F. Harrison, D.H. Perkins and W.G. Scott, *Tri-bimaximal mixing and the neutrino oscillation data*, *Phys. Lett. B* **530** (2002) 167 [[hep-ph/0202074](#)].
- [34] P.F. Harrison and W.G. Scott, *Symmetries and generalizations of tri - bimaximal neutrino mixing*, *Phys. Lett. B* **535** (2002) 163 [[hep-ph/0203209](#)].
- [35] DAYA BAY collaboration, *Observation of electron-antineutrino disappearance at Daya Bay*, *Phys. Rev. Lett.* **108** (2012) 171803 [[1203.1669](#)].
- [36] RENO collaboration, *Observation of Reactor Electron Antineutrino Disappearance in the RENO Experiment*, *Phys. Rev. Lett.* **108** (2012) 191802 [[1204.0626](#)].
- [37] G.C. Branco, R. Gonzalez Felipe, F.R. Joaquim and H. Serodio, *Spontaneous leptonic CP violation and nonzero θ_{13}* , *Phys. Rev. D* **86** (2012) 076008 [[1203.2646](#)].
- [38] C.-C. Li, J.-N. Lu and G.-J. Ding, *A_4 and CP symmetry and a model with maximal CP violation*, *Nucl. Phys. B* **913** (2016) 110 [[1608.01860](#)].
- [39] T. Araki, J. Mei and Z.-z. Xing, *Intrinsic Deviation from the Tri-bimaximal Neutrino Mixing in a Class of A_4 Flavor Models*, *Phys. Lett. B* **695** (2011) 165 [[1010.3065](#)].
- [40] N. Memenga, W. Rodejohann and H. Zhang, *A_4 flavor symmetry model for Dirac neutrinos and sizable U_{e3}* , *Phys. Rev. D* **87** (2013) 053021 [[1301.2963](#)].
- [41] D. Borah and B. Karmakar, *A_4 flavour model for Dirac neutrinos: Type I and inverse seesaw*, *Phys. Lett. B* **780** (2018) 461 [[1712.06407](#)].
- [42] D. Borah, B. Karmakar and D. Nanda, *Common Origin of Dirac Neutrino Mass and Freeze-in Massive Particle Dark Matter*, *JCAP* **07** (2018) 039 [[1805.11115](#)].
- [43] D. Borah and B. Karmakar, *Linear seesaw for Dirac neutrinos with A_4 flavour symmetry*, *Phys. Lett. B* **789** (2019) 59 [[1806.10685](#)].
- [44] G. Branco, R. Gonzalez Felipe, M. Rebelo and H. Serodio, *Resonant leptogenesis and tribimaximal leptonic mixing with $A(4)$ symmetry*, *Phys. Rev. D* **79** (2009) 093008 [[0904.3076](#)].
- [45] M. Fukugita and T. Yanagida, *Baryogenesis Without Grand Unification*, *Phys. Lett. B* **174** (1986) 45.

- [46] M.A. Luty, *Baryogenesis via leptogenesis*, *Phys. Rev. D* **45** (1992) 455.
- [47] M. Plumacher, *Baryogenesis and lepton number violation*, *Z. Phys. C* **74** (1997) 549 [[hep-ph/9604229](#)].
- [48] L. Covi, E. Roulet and F. Vissani, *CP violating decays in leptogenesis scenarios*, *Phys. Lett. B* **384** (1996) 169 [[hep-ph/9605319](#)].
- [49] A. Datta, R. Roshan and A. Sil, *Imprint of the seesaw mechanism on feebly interacting dark matter and the baryon asymmetry*, [2104.02030](#).
- [50] D. Borah, M.K. Das and A. Mukherjee, *Common origin of nonzero θ_{13} and baryon asymmetry of the Universe in a TeV scale seesaw model with A_4 flavor symmetry*, *Phys. Rev. D* **97** (2018) 115009 [[1711.02445](#)].
- [51] B. Karmakar and A. Sil, *Nonzero θ_{13} and leptogenesis in a type-I seesaw model with A_4 symmetry*, *Phys. Rev. D* **91** (2015) 013004 [[1407.5826](#)].
- [52] B. Karmakar and A. Sil, *Spontaneous CP violation in lepton-sector: A common origin for θ_{13} , the Dirac CP phase, and leptogenesis*, *Phys. Rev. D* **93** (2016) 013006 [[1509.07090](#)].
- [53] S. Bhattacharya, B. Karmakar, N. Sahu and A. Sil, *Unifying the flavor origin of dark matter with leptonic nonzero θ_{13}* , *Phys. Rev. D* **93** (2016) 115041 [[1603.04776](#)].
- [54] S. Bhattacharya, B. Karmakar, N. Sahu and A. Sil, *Flavor origin of dark matter and its relation with leptonic nonzero θ_{13} and Dirac CP phase δ* , *JHEP* **05** (2017) 068 [[1611.07419](#)].
- [55] C. Hagedorn, E. Molinaro and S.T. Petcov, *Majorana Phases and Leptogenesis in See-Saw Models with $A(4)$ Symmetry*, *JHEP* **09** (2009) 115 [[0908.0240](#)].
- [56] E.E. Jenkins and A.V. Manohar, *Tribimaximal Mixing, Leptogenesis, and $\theta(13)$* , *Phys. Lett. B* **668** (2008) 210 [[0807.4176](#)].
- [57] P. Das, M.K. Das and N. Khan, *Phenomenological study of neutrino mass, dark matter and baryogenesis within the framework of minimal extended seesaw*, *JHEP* **03** (2020) 018 [[1911.07243](#)].
- [58] A. Pilaftsis, *CP violation and baryogenesis due to heavy Majorana neutrinos*, *Phys. Rev. D* **56** (1997) 5431 [[hep-ph/9707235](#)].
- [59] B. Karmakar and A. Sil, *An A_4 realization of inverse seesaw: neutrino masses, θ_{13} and leptonic non-unitarity*, *Phys. Rev. D* **96** (2017) 015007 [[1610.01909](#)].
- [60] X.-G. He, Y.-Y. Keum and R.R. Volkas, *$A(4)$ flavor symmetry breaking scheme for understanding quark and neutrino mixing angles*, *JHEP* **04** (2006) 039 [[hep-ph/0601001](#)].
- [61] Y. Lin, *A Predictive $A(4)$ model, Charged Lepton Hierarchy and Tri-bimaximal Sum Rule*, *Nucl. Phys. B* **813** (2009) 91 [[0804.2867](#)].
- [62] W. Rodejohann and X.-J. Xu, *A left-right symmetric flavor symmetry model*, *Eur. Phys. J. C* **76** (2016) 138 [[1509.03265](#)].
- [63] PARTICLE DATA GROUP collaboration, *Review of Particle Physics*, *Phys. Rev. D* **98** (2018) 030001.
- [64] I. Esteban, M. Gonzalez-Garcia, M. Maltoni, T. Schwetz and A. Zhou, *The fate of hints: updated global analysis of three-flavor neutrino oscillations*, *JHEP* **09** (2020) 178 [[2007.14792](#)].

- [65] P. Langacker, S.T. Petcov, G. Steigman and S. Toshev, *On the Mikheev-Smirnov-Wolfenstein (MSW) Mechanism of Amplification of Neutrino Oscillations in Matter*, *Nucl. Phys. B* **282** (1987) 589.
- [66] S. Vagnozzi, E. Giusarma, O. Mena, K. Freese, M. Gerbino, S. Ho et al., *Unveiling ν secrets with cosmological data: neutrino masses and mass hierarchy*, *Phys. Rev. D* **96** (2017) 123503 [[1701.08172](#)].
- [67] PLANCK collaboration, *Planck 2018 results. VI. Cosmological parameters*, *Astron. Astrophys.* **641** (2020) A6 [[1807.06209](#)].
- [68] A. Ilakovac and A. Pilaftsis, *Flavor violating charged lepton decays in seesaw-type models*, *Nucl. Phys. B* **437** (1995) 491 [[hep-ph/9403398](#)].
- [69] D. Tommasini, G. Barenboim, J. Bernabeu and C. Jarlskog, *Nondecoupling of heavy neutrinos and lepton flavor violation*, *Nucl. Phys. B* **444** (1995) 451 [[hep-ph/9503228](#)].
- [70] S. Bhattacharya, R. Roshan, A. Sil and D. Vatsyayan, *Symmetry origin of Baryon Asymmetry, Dark Matter and Neutrino Mass*, [2105.06189](#).
- [71] S.Y. Khlebnikov and M.E. Shaposhnikov, *The Statistical Theory of Anomalous Fermion Number Nonconservation*, *Nucl. Phys. B* **308** (1988) 885.
- [72] P.B. Arnold and L.D. McLerran, *The Sphaleron Strikes Back*, *Phys. Rev. D* **37** (1988) 1020.
- [73] B. Adhikary, M. Chakraborty and A. Ghosal, *Flavored leptogenesis with quasidegenerate neutrinos in a broken cyclic symmetric model*, *Phys. Rev. D* **93** (2016) 113001 [[1407.6173](#)].
- [74] A. Pilaftsis and T.E.J. Underwood, *Resonant leptogenesis*, *Nucl. Phys.* **B692** (2004) 303 [[hep-ph/0309342](#)].
- [75] P.S.B. Dev, M. Garny, J. Klaric, P. Millington and D. Teresi, *Resonant enhancement in leptogenesis*, *Int. J. Mod. Phys. A* **33** (2018) 1842003 [[1711.02863](#)].
- [76] J. Casas, J. Espinosa, A. Ibarra and I. Navarro, *Naturalness of nearly degenerate neutrinos*, *Nucl. Phys. B* **556** (1999) 3 [[hep-ph/9904395](#)].
- [77] R. Gonzalez Felipe, F. Joaquim and B. Nobre, *Radiatively induced leptogenesis in a minimal seesaw model*, *Phys. Rev. D* **70** (2004) 085009 [[hep-ph/0311029](#)].
- [78] P.H. Chankowski and S. Pokorski, *Quantum corrections to neutrino masses and mixing angles*, *Int. J. Mod. Phys. A* **17** (2002) 575 [[hep-ph/0110249](#)].
- [79] M. Flanz, E.A. Paschos, U. Sarkar and J. Weiss, *Baryogenesis through mixing of heavy Majorana neutrinos*, *Phys. Lett. B* **389** (1996) 693 [[hep-ph/9607310](#)].
- [80] S. Pascoli, S. Petcov and A. Riotto, *Leptogenesis and Low Energy CP Violation in Neutrino Physics*, *Nucl. Phys. B* **774** (2007) 1 [[hep-ph/0611338](#)].
- [81] A. Abada, S. Davidson, F.-X. Josse-Michaux, M. Losada and A. Riotto, *Flavor issues in leptogenesis*, *JCAP* **04** (2006) 004 [[hep-ph/0601083](#)].
- [82] J.M. Cline, K. Kainulainen and K.A. Olive, *Protecting the primordial baryon asymmetry from erasure by sphalerons*, *Phys. Rev. D* **49** (1994) 6394 [[hep-ph/9401208](#)].
- [83] A. Abada, S. Davidson, A. Ibarra, F.X. Josse-Michaux, M. Losada and A. Riotto, *Flavour Matters in Leptogenesis*, *JHEP* **09** (2006) 010 [[hep-ph/0605281](#)].
- [84] E. Nardi, Y. Nir, E. Roulet and J. Racker, *The Importance of flavor in leptogenesis*, *JHEP* **01** (2006) 164 [[hep-ph/0601084](#)].

- [85] E. Nardi, Y. Nir, J. Racker and E. Roulet, *On Higgs and sphaleron effects during the leptogenesis era*, *JHEP* **01** (2006) 068 [[hep-ph/0512052](#)].
- [86] T. Asaka and T. Yoshida, *Resonant leptogenesis at TeV-scale and neutrinoless double beta decay*, *JHEP* **09** (2019) 089 [[1812.11323](#)].
- [87] M. Plümacher, *Baryon asymmetry, neutrino mixing and supersymmetric SO(10) unification*, Ph.D. thesis, Hamburg U., 1998. [hep-ph/9807557](#). 10.3204/PUBDB-2016-02633.